

Late Quaternary dextral surface fault offset and neotectonic geomorphology at a locality on the NW segment of the Sargent fault, Santa Clara County, California

Frank J. Groffie¹, March 14, 2019

Abstract

The Sargent fault is known to extend 54 km between a connection with the San Andreas fault on the northwest and a possible connection with the Calaveras fault on the southeast. Seismicity and Holocene surface rupture have been well documented on all three faults. Holocene activity on the southeast segment of the Sargent fault has been reported, but previous reports of large-scale late Quaternary surface offset on its northwest segment have been vague. There is a locality on the northwest segment of the Sargent fault that hosts a previously unrecognized set of neotectonic geomorphic features including a shutter ridge, beheaded stream, hanging valley, aligned overhanging cliffs, and contorted microtopography. Detailed field mapping of these features and the underlying geology indicates that about 75 m of purely dextral latest Quaternary (latest Pleistocene and likely Holocene) surface offset, spanning a time period of about 25 ky, occurred on the Sargent fault at this locality. These findings provide the first field quantification of large-scale late Quaternary surface offset on this fault segment. In contrast with earlier reporting and mapping, the fault here is exposed at the ground surface, its trace can be spatially constrained to a zone 1 m to a few meters wide locally, and its latest sense of Quaternary slip is mainly dextral. The field data lend support to a previously reported recurrence interval of 1200 yr and a previously conjectured fault dip to the northeast.

Keywords: Sargent fault, surface fault offset, neotectonic, geomorphology, Santa Clara County

1. Study area

A set of previously unrecognized, closely spaced neotectonic geomorphic features on the Sargent fault is located within a roughly 300-m-long locality where Swanson Creek flows into Uvas Creek. This locality, hereafter referred to as the *Swanson locality*, is centered on Lower Swanson Creek Falls, at the coordinates lat. 37.0857 N by long. -121.7927 W, at an elevation of 330 m (1000 ft.) above sea level. The locality is at 8515 Croy Road, in Santa Clara County, California, 29 km south of the city of San Jose (Fig. 1).

The Swanson locality is located mostly within Uvas Canyon County Park, which is administered by the Santa Clara County Department of Parks and Recreation. Land north of the park belongs to the Santa Clara County Open Space Authority. Land to the east belongs to the Swedish American Patriotic League and is occupied by the village of Sveadal, which is a small private community that serves as a summer resort.

The Swanson locality is accessed by driving to the end of Croy Road within the park and walking down Swanson Creek Trail to its end at Lower Swanson Creek Falls. Alternately, one can walk down Uvas Creek Trail to where it also ends at the falls. The two trails do not connect at the falls due to the rugged terrain there and the lack of a bridge or other permanent safe passage for hikers across the creeks. During times of low stream flow, however, one may be able to travel from one trail to the other by a combination of crossing(s) of one or both streams and ascending/descending an extremely steep slope.

2. Geologic setting

The Swanson locality is located in the Santa Cruz Mountains, which are one range in a series of basins and ranges in the Coast Ranges of California (Fig. 1). The geology of this region is characterized by small northwest-oriented structural blocks bounded by numerous anastomosing northwest-trending faults. According to Graymer (1997), “each structural block contains a distinct stratigraphic sequence, ... and ... large-scale movement on the block-bounding faults has juxtaposed the rocks in each.” The Swanson locality is situated on the Sierra Azul block, which is bounded by the San Andreas fault (SAF) on the southwest and the Sargent fault on the northeast (Graymer, 1997). This block is generally composed of tightly folded Cretaceous and Tertiary strata.

The block-bounding faults are part of the SAF system, which forms the boundary between the Pacific and North American plates. Several of these faults (SAF and Calaveras and Sargent faults) have been active during the Neogene and Quaternary, including historic time (Fig. 1).

The Sargent fault extends 54 km (Bryant, 2000a, b) between a connection with the SAF on the northwest and a likely connection with the Calaveras fault on the southeast (Fig. 1). Bryant (2000a, b) informally divided the Sargent fault, at about its midpoint at Hecker Pass, into a northwest segment and southeast segment,² hereinafter referred to as the *Sargent fault NWS* and *Sargent fault SES*, respectively.

¹ Free-lance consultant, office in San Jose, California. www.groffie.com. Contact at fgroffie@aol.com, 408-314-8237. The author earned a B.S. in geology from the University of California, Berkeley, and an M.A. in geological science from San Diego State University and is a State of California professional geologist (No. 4930) and certified engineering geologist (No. 1539).

² This fault segmentation is informal (Bryant, 2000a, b) and may have no seismological basis or implications.

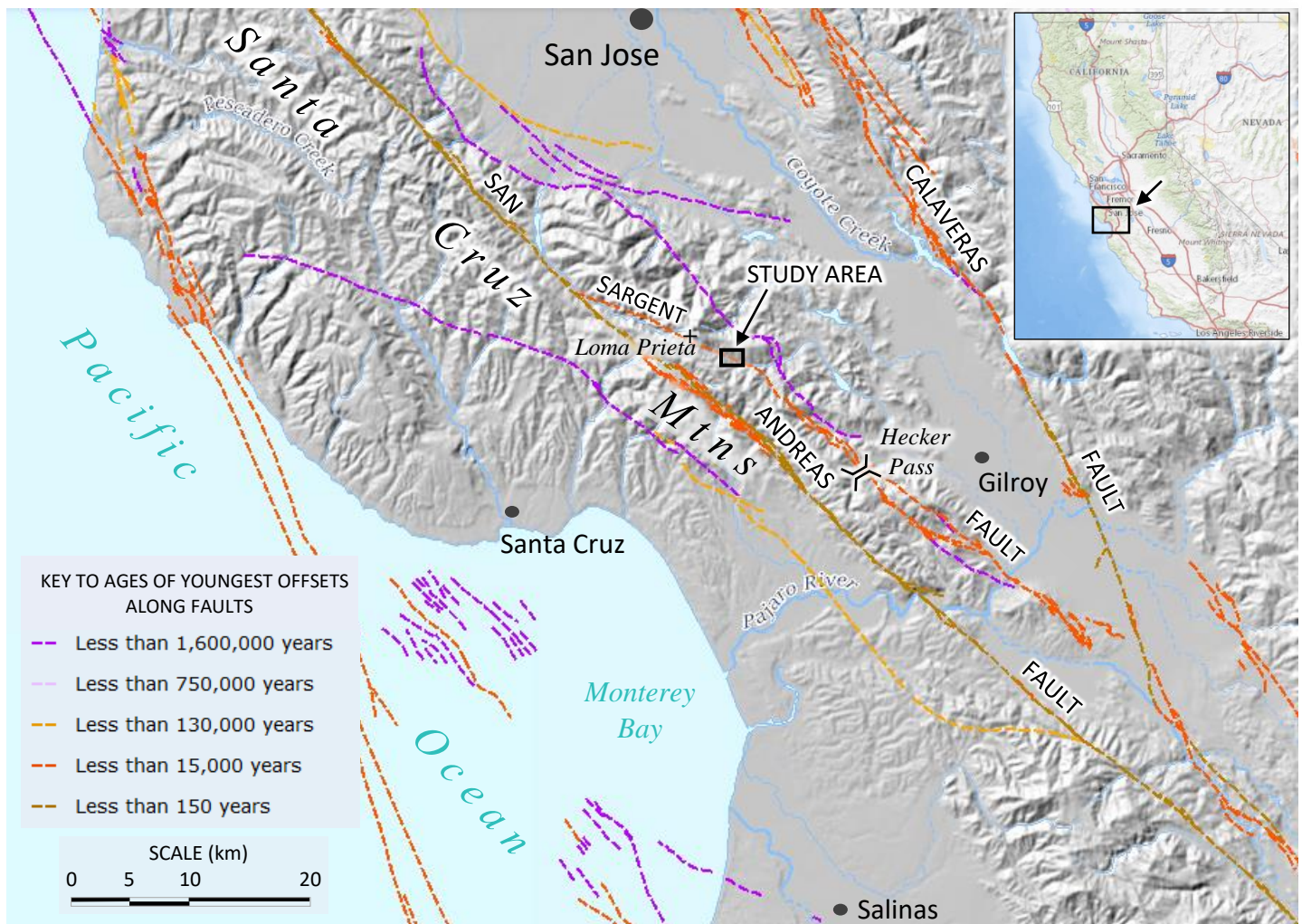


Figure 1. Map showing study area and Quaternary faults in the region. Base map prepared using the U.S. Geological Survey’s GIS application <https://viewer.nationalmap.gov/advanced-viewer/>. Fault age-of-offset legend from <https://usgs.maps.arcgis.com/home/item.html?id=4c1411f4fd324a77b20dc5e138d4baf0>, updated February 2018. Labels of selected geographic features and fault traces added.

3. Local topography

The topography of the study area is dominated by Uvas Creek, a perennial stream that flows eastward through the study area (Fig. 2). The hillsides on either side are generally steep and are dissected by numerous small streams. Swanson Creek is a perennial stream that flows northwestward to its confluence with Uvas Creek at the Swanson locality.

What was once a single broad, high stream terrace in this area has been dissected by Swanson Creek, both its active and beheaded portions (Fig. 2). The portion of terrace on the northwest side of the creek is occupied by the campground of Uvas Canyon County Park, and the portion to the southeast is occupied by the park office and the community of Sveadal. Hence, these two segments of terrace are herein designated the *campground terrace* and the *park office terrace* (Fig. 2). Surface fault offset and a paleowaterfall/cascade have created a small hanging valley in the middle of the Swanson locality (Fig. 2).

4. Historic land use

According to Santa Clara County Parks (2015), settlers of European descent first settled in Uvas Canyon in 1865 and began to build homes, cut timber (redwood and Douglas fir), mill lumber, and plant vineyards and orchards. The area that is now Sveadal (Fig. 3) was homesteaded in about 1887. In 1926, certain holdings were sold to the Swedish American Patriotic League, which encouraged development of the property with vacation cabins, resulting in the community of Sveadal. The land to the west, around Swanson Creek, was homesteaded by others in the late 19th century. This land was sold to the Santa Clara County parks department in 1961, and in 1962, Uvas Canyon County Park was opened to the public.

Human disturbance can obscure neotectonic features, and old unpaved roads and building pads can be misidentified as natural features. Historic maps and aerial photographs were reviewed (Appendix) and field mapping was performed to minimize confusion of anthropogenic and natural geomorphic

features. Thus, the geomorphic features described in Section 7 all appear to be natural rather than anthropogenic.

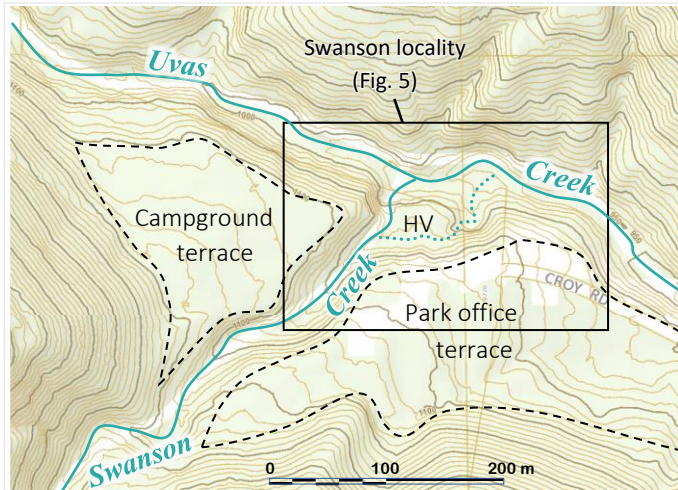


Figure 2. Topographic map of study area, showing two principal terrace trends. Base is from Santa Clara County et al. (2017). Perennial streams (solid blue lines) and beheaded portion of Swanson Creek (dotted blue line) were added. HV = hanging valley. Contour interval is 10 ft. (3.3 m).

5. Previous geological and seismological work

The geology of areas that include the Swanson locality has been mapped by several investigators in the previous five decades. Mapping of the pre-Quaternary stratigraphy in the study area by other investigators has varied. The pre-Quaternary exposures have been variably assigned to Jurassic–Cretaceous basalt, Cretaceous marine units (Panoche Formation or unassigned), and Tertiary marine units. Rather than attempt to resolve these differences, the discussion below focuses on the areal distribution of Quaternary alluvial deposits and on the mapping of the Sargent fault.

Dibblee and Brabb (1980), McLaughlin et al. (1988), Wentworth et al. (1999), McLaughlin et al. (2001), McLaughlin et al. (2004), and Dibblee and Minch (2005) produced geologic maps of parts of the Santa Cruz Mountains that include the study area. These maps all show an area around the confluence of Swanson and Uvas Creeks, i.e., the study area, as underlain by a laterally extensive deposit of Quaternary alluvium (Fig. 3). The maps do not distinguish between alluvial deposits of various ages underlying different geomorphic surfaces. They also all show the Sargent fault as concealed beneath (i.e., pre-dating, not offsetting) this Quaternary alluvium. Evidently, then, no exposures or other well-defined features marking the trace of the fault were recognized at the Swanson locality.

Mapping of the Sargent fault NWS was first performed in detail by McLaughlin (1973, 1974), who also first reported Quaternary activity along the fault. The Sargent fault is fre-

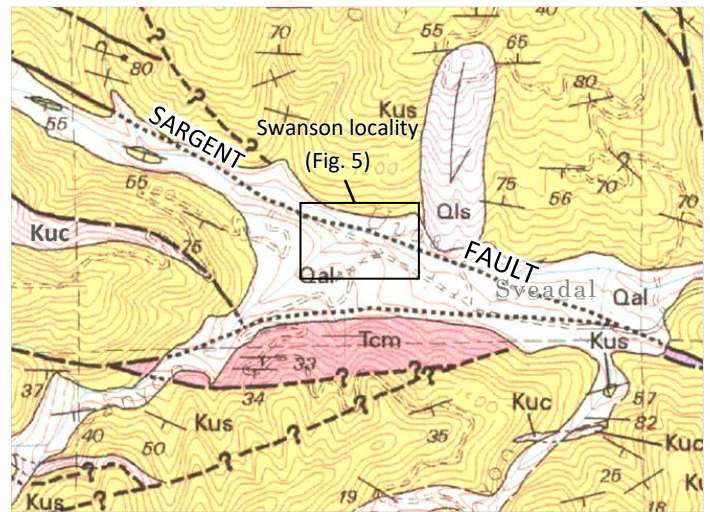


Figure 3. Portion of geologic map by McLaughlin et al. (2001). Note Sargent fault (label added) concealed beneath laterally extensive undifferentiated alluvium. Kus = Cretaceous sandstone, Kuc = Cretaceous conglomerate, Tcm = Tertiary mudstone, Qls = Quaternary landslide, Qal = Quaternary alluvium.

quently described as connecting at depth with the SAF, and the Sargent fault NWS has frequently been described as a south-west-dipping reverse fault with an unknown component of strike slip (e.g., McLaughlin et al., 2001).

Recently, based on seismic-reflection and earthquake-hypocenter data, Zhang et al. (2018) concluded that the Sargent fault dips steeply to the northeast at depths shallower than about 2 km (Fig. 4). McLaughlin et al. (1997) speculated that the Sargent fault zone could account for as much as 26 km of dextral slip. According to McLaughlin et al. (2001), offset along the Sargent fault may have been predominantly strike slip “during the latest stages of its offset history,” i.e., “later than 10 Ma.”

Quaternary and historic activity on the Sargent fault has been reported in detail but primarily on the fault’s southeast segment. Prescott and Burford (1976) analyzed survey results from the years 1970–75 from a trilateration net that straddled the Sargent fault SES and was located about 16 km southeast of the Swanson locality. They obtained an estimated historic slip rate of about 3 mm/yr. Nolan et al. (1995) performed trench exploration 29 km southeast of the Swanson locality (i.e., on the Sargent fault SES). They concluded that four offsets of Holocene floodplain deposits had occurred along the fault in the past 5940 yr, indicating an average recurrence interval of about 1485 yr, and that the most-recent offset occurred sometime after 2940 yr BP. WGNCEP (1996) and Petersen et al. (1996) assigned the fault recurrence intervals of 330 yr and 1200 yr, respectively.

Kilb and Hardebeck (2006) analyzed microearthquakes along the Sargent fault SES that were cataloged between 1984 and 1997. They assigned 655 events, with a median magnitude of

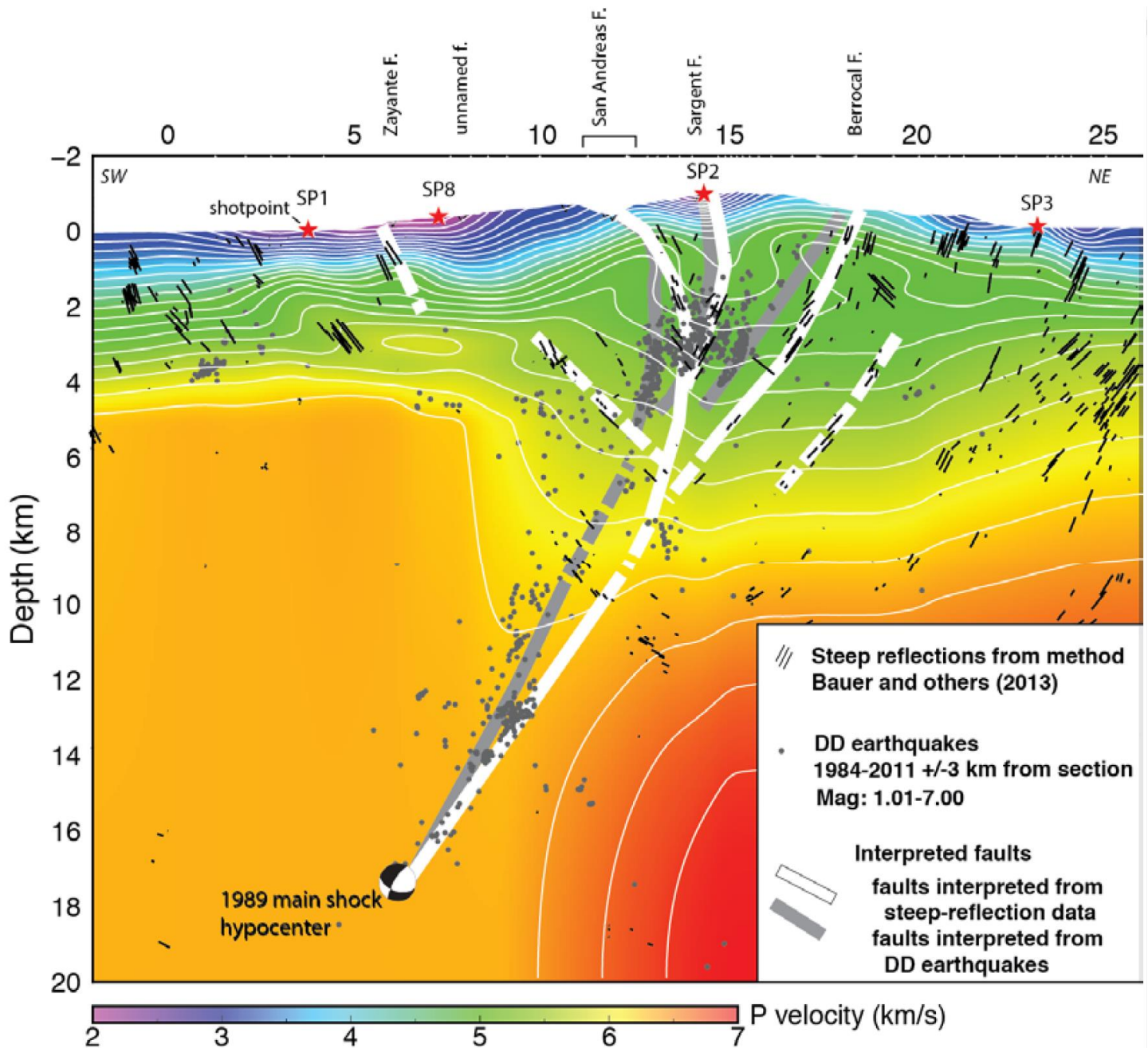


Figure 4. Interpretations of subsurface fault geometries through the Loma Prieta profile by Zhang et al. (2018); cover illustration in that paper. Profile location is located 17 km northwest of the Swanson locality. Note the conjectured northeastward dip of the Sargent fault above a 2-km depth and the fault's connection with the SAF at a 5–6-km depth. Mag. = magnitude, DD earthquakes = earthquake hypocenters relocated using double-difference and waveform cross-correlation methods, P = compressional wave, main shock is that of the 1989 Loma Prieta earthquake.

1.1, to the fault. They assigned the following geometric parameters to this fault segment: strike of N46°W, dip of 87°NE (essentially vertical), and an assumed horizontal (strike-slip) slip vector.

Turner et al. (2013) documented seismic activity along the Sargent fault based on earthquakes in the aftershock zone of the 1989 Loma Prieta earthquake. These authors, in their dis-

cussion of the Sargent fault SES, concluded that beginning in 1998, there was

a gradual ramp-up of activity on the Sargent fault and the start of a temporal correlation of slip rate variations on the two faults [Sargent and San Andreas] in which they begin periodically rising and falling together. These observations imply

that the faults share a common driving or weakening mechanism.

Compared to the southeast segment, the Sargent fault NWS has received little attention. During the 1989 Loma Prieta earthquake, ground surface rupture, including 10 cm of dextral displacement, occurred on the 2.4 km of the fault where it connects with the SAF (McLaughlin and Clark, 2004). Dietz and Ellsworth (1990) analyzed data from the Loma Prieta earthquake rupture zone, a portion of which parallels most of the Sargent fault, including its northwest segment. They proposed several models in which the 3-D aftershock pattern following this earthquake was assigned to the SAF and regional branches. In one model, the earthquake rupture occurred on the southwest-dipping SAF up to a depth of 6 km and continued upward on a southwest-dipping Sargent fault up to a depth of about 3½ km. The data, however, “fail to support an association with the Sargent fault”.

WGNCEP (1996), in a discussion of the northern third(?) of the Sargent fault, concluded the following:

Evidence for recency is more obscure in the steep and heavily vegetated terrain to the north where a larger dip-slip component is required to accommodate volume problems at the junction with the San Andreas fault.

Bryant (2000a) summarized what was known of recent activity along the Sargent fault NWS. His summarization included the following notes:

Timing of the most recent paleoevent is unknown. However, the geomorphic expression of the fault zone is suggestive of latest Pleistocene to Holocene displacement Late Quaternary displacement is indicated by captured drainages and linear troughs (McLaughlin, 1974 ...).

A possible explanation for the relative lack of information regarding the Sargent fault NWS may be the limited scale of previous mapping of its trace and the associated geomorphology. The emphasis may have been on identifying evidence of dip-slip displacement along the Sargent fault. Consequently, the remarkable features indicating strike-slip displacement at the Swanson locality evidently were overlooked. The findings and discussions in Sections 6 through 9, below, serve to fill in this information gap.

6. Local geology

Geologic units mapped within the Swanson locality, as shown in Fig. 5, listed from oldest to youngest, are Cretaceous sandstone, an extensive Pleistocene alluvial terrace deposit, two units consisting of localized late Pleistocene to Holocene alluvial deposits, recent active alluvium, and at least one small landslide deposit. The Sargent fault passes through the study area. Here, the fault has strongly controlled the distribution of bedrock exposures and alluvial deposits and the topography.

Cretaceous sandstone. Bedrock at the locality consists of Cretaceous sandstone, herein unassigned to any formal stratigraphic unit (map symbol *Kus* in Fig. 5). This stratigraphic designation is based on mapping by previous workers (Section 5), particularly, that of McLaughlin et al. (2001) and Dibblee and Minch (2005). This Cretaceous sandstone unit is exposed alongside Uvas Creek and at Lower Swanson Creek Falls (Fig. 5). The unit consists mostly of massive, very fine-grained, lithic sandstone. The sandstone beds, of undetermined thickness, appear to be devoid of macroscopic internal bedding. The unit also contains minor conglomeratic lenses (Fig. 6) containing rounded clasts up to 10 cm in diameter and minor fissile, flaky shale lenses. These minor conglomerate and shale lenses make up some 20% of the unit locally, and the shale lenses yield the only few, scattered bedding attitudes in the unit. Local bedding within the unit tends to dip steeply to the north, consistent with mapping across a larger area by McLaughlin et al. (2001). Much of this unit is covered with slopewash derived from unit Qoa₁.



Figure 6. Conglomerate in unit Kus.

Unit Qoa₁. The oldest Quaternary alluvial deposit (Qoa₁) underlies the extensive stream terraces at about Elev. 1100 ft, i.e., the campground terrace and park office terrace. There are also three small prominent remnants on the north side of the hanging valley. The maximum thickness of this unit is about 25 m. Its lower contact with the underlying Cretaceous sandstone bedrock is an angular unconformity that likely dips gently eastward toward Uvas Creek. The lower contact is well exposed at about the 1020-ft-contour next to the falls (Fig. 13) and where Swanson Creek Trail exits the east end of the hanging valley. The ground underlain by the unit is generally that of an alluvial fan sloping northward to eastward toward Uvas Creek at an overall gradient of about 4–5% (Fig. 2) but is significantly dissected and warped by some combination of erosion and tectonism. The unit generally consists of bouldery gravel and sand (Fig. 7). The boulders are composed of sandstone, conglomerate, and shale derived from the underlying

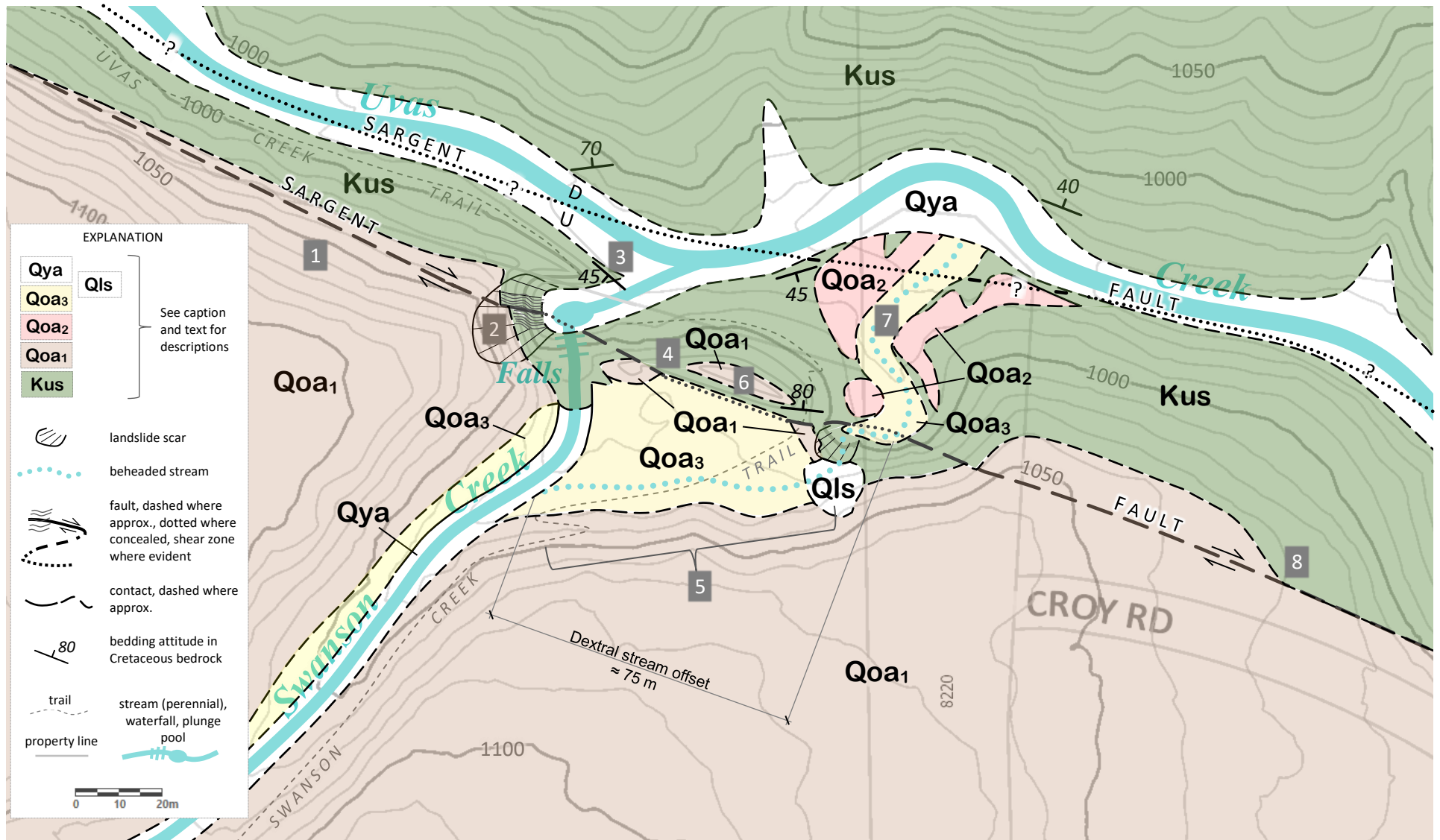


Figure 5. Geologic map of Swanson locality, including neotectonic features. Base map is from Santa Clara County et al. (2017), modified by alteration of contours to clearly depict shutter ridge(s) and by addition of contour labels, creeks, falls, and trails. Elevations are feet above mean sea level. Contour interval is 10 ft (3.3 m). Kus = Cretaceous unnamed sandstone, Qoa₁ = oldest Quaternary alluvial terrace deposit, Qoa₂ = Quaternary alluvium associated with rejuvenated paleo-Swanson Creek, Qoa₃ = Quaternary alluvium associated with latest activity of paleo-Swanson Creek, Qya = active alluvium associated with modern perennial creeks, Qls = Quaternary landslide deposit. The southwestern branch of the Sargent fault shown here is the principle young trace of the Sargent fault with dextral offset, and other minor late Quaternary dextral fault traces may be present. Numbers 1 through 8 are keyed to descriptions of neotectonic features in the text. Also shown are dimensioning lines used to estimate total dextral stream offset.

Cretaceous sandstone, are generally rounded, and range in size up to 3 m across. The unit's internal structure is generally one



Figure 7. Typical exposure of unit Qoa₁. Camera case for scale.

of disorganized deposition devoid of bedding and tending more toward matrix support rather than clast support. These sedimentologic features suggest deposition by debris flows. An exception is near the base of the unit, which is well exposed next to the falls, where the unit displays relatively well-developed bedding involving silt, sand, and gravel (Fig. 8). Some of the clasts display in-place weathering (softened, fragile consistencies) (Fig. 9). The matrix of sand and minor silt and clay gives the unit a distinct brown color (typically 7½YR 4/4) in roadcut and streamcut exposures.



Figure 8. Stratification at base of unit Qoa₁ exposed in a streamcut (with undercutting) produced by Swanson Creek, viewed looking west.

Unit Qoa₂. A second unit of Quaternary alluvium (Qoa₂) underlies a set of small isolated topographic humps alongside the lower beheaded segment of Swanson Creek. The thickness of these deposits appears to be about 2½ m. The lower contact



Figure 9. Small remnant of unit Qoa₁ at east end of hanging valley, exposed in small landslide scarp. Scale (18 cm long) lies next to a rounded, matrix-supported, weathered-in-place cobble.

is an angular unconformity developed on the Kus bedrock. The rounded, lobate shapes of the bodies and their lateral distribution suggest that deposition was by debris flows that formed a small alluvial fan at the paleoconfluence of Swanson and Uvas Creeks. The material composing unit Qoa₂ likely was derived primarily from the dissection of unit Qoa₁ by Swanson Creek. The texture and internal structure of unit Qoa₂ (Fig. 10) are similar to those of unit Qoa₁ except that the boulders tend to be smaller, i.e., less than 2 m in diameter, and the sand matrix contains essentially no clay and feels looser. A few of the rounded shale cobbles show signs of in-place weathering (slaking; Fig. 11). The matrix of sand gives the unit a brown color (7½YR 3/3) that tends to be slightly weaker and darker than that of unit Qoa₁. The unit's distribution as isolated bodies indicates later dissection by the beheaded segment of Swanson Creek.

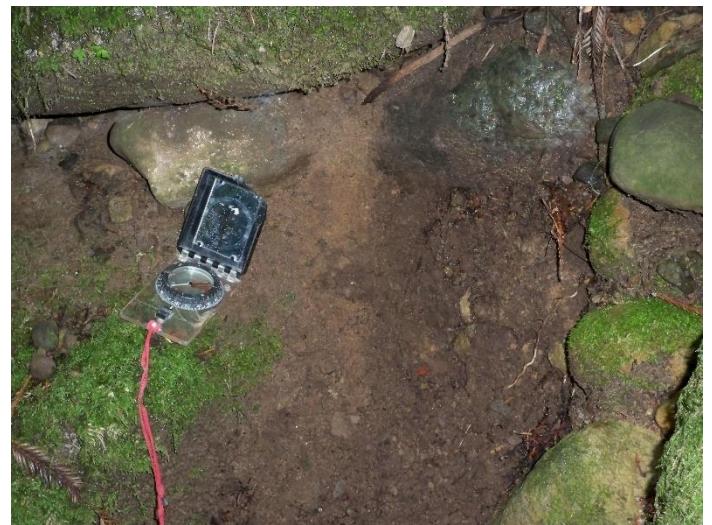


Figure 10. Typical exposure of unit Qoa₂.



Figure 11. Weathered-in-place (slaked) shale cobble in unit Qoa₂.

Unit Qoa₃. A third unit of Quaternary deposits (Qoa₃) underlies the beheaded portion of Swanson Creek, both within the hanging valley and below, and a narrow terrace alongside active Swanson Creek. The unit's maximum thickness is about 2 m. The unit clearly overlaps unit Qoa₁ above Swanson Creek falls and overlaps unit Qoa₂ and Kus bedrock elsewhere. The unit's upper surface is planar to slightly hummocky, as if transport occurred mainly as bedload and suspended load and secondarily as debris flows. In the middle of the hanging valley, there are two unusual manmade features: an old steel barrel that is mostly buried within the alluvium (Fig. 12), and the end of an iron pipe that protrudes a few centimeters above



Figure 12. Enigmatic steel barrel mostly buried within unit Qoa₃ in the hanging valley. In contrast with modern steel barrels made with integral stamped ribs, for rigidity and easy rolling, this ~200-liter barrel was made with a smooth cylindrical face and two external steel hoops, suggesting that it was manufactured around 1900. Camera case for scale.

the ground surface. The material within and surrounding the barrel consists of a 6-cm-thick layer of leaf litter underlain by brownish-gray, loose, well-sorted medium-grained sand. Several trees, whose trunks are all about $\frac{1}{3}$ to $\frac{1}{2}$ m or slightly less in diameter, are growing on the floor of the hanging valley. Thus, the youngest alluvium may have been deposited by Swanson Creek in the early 20th century. Afterward, the active segment of Swanson Creek clearly dissected this unit.

Active alluvium. A unit consisting of young alluvium (Qya), active during historic time, lines the active channels of Uvas and Swanson Creeks. Its thickness is typically $\frac{1}{2}$ to 1 m. It generally consists of rounded gravel including boulders up to 3 m across. The largest boulders may have been derived from unit Qoa₁ and been transported only short distances. The clasts are generally rounded sandstone and conglomerate derived from unit Kus.

Sargent fault. The Sargent fault passes northwestward through the Swanson locality as shown in Fig. 5. At Lower Swanson Creek Falls, what is likely the principle youngest trace of the Sargent fault is located within a shear zone about 8 m thick consisting of fissile, sheared, platy shale (Fig. 13).¹

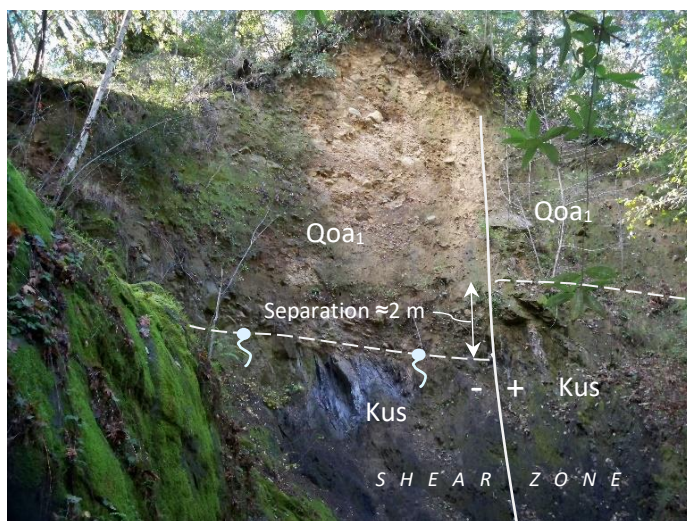


Figure 13. Principle young(est?) trace of Sargent fault, exposed in eroded bowl adjacent to Lower Swanson Creek Falls, viewed looking west. Height of the cliff in this view is about 10 m. Interpretations, based on viewing through binoculars, are as follows: dashed subhorizontal lines denote the contact between Cretaceous sandstone (Kus) below and unit Qoa₁ above; solid vertical line denotes the fault trace, along which there is vertical fault separation of the contact of about 2 m (NE [right] side “up”); and traditional symbols schematically represent numerous spring flows observed emanating from the contact in early 2019. Purely dextral fault slip is assumed, denoted by + and – symbols. Note the dark-gray rock of the shear zone within unit Kus and, within, the shear planes dipping steeply northeast. The moss-covered slope in the lower left corner is a tall bedrock outcrop in the foreground that, in this view, hides the falls.

¹ This shear zone was not observed southeast of the falls because there it either is not present (pinches out), is covered by slopewash,

or is too difficult to access and observe (due to the waterfall and unsafe footing).

This fault strikes about N70°W, based on the shear planes observed near the falls and the neotectonics features elsewhere within the Swanson locality.

Fig. 13 shows where the principle young(est?) trace of the Sargent fault has offset unit Qoa₁. This exposure has produced a NE-side-up vertical separation of the Kus–Qoa₁ contact of about 2 m along this fault trace. That sense of separation would be the opposite produced by a SW-side-up dip-slip component of displacement on the Sargent fault shown on all previous maps of the area. Thus, latest Pleistocene to Holocene dip slip on the Sargent fault NWS apparently was negligible, and primarily or purely strike-slip latest Quaternary displacement should be assumed. Based on this assumed purely dextral slip, then, the vertical separation is perpendicular to the slip vector and was produced by juxtaposition of a Kus–Qoa₁ contact formerly located farther west and at a higher elevation against a lower-elevation Kus–Qoa₁ contact at the falls. Assuming that the Kus–Qoa₁ contact slopes about 4% eastward, as does Uvas Creek here, and given the 75 m of purely dextral fault slip shown in Fig. 5, a NE-side-up vertical separation of the contact of about 2½ m would be predicted at the falls. A similar vertical fault separation (~3 m) can be observed about 40 m to the east, as described later (Feature 6, in Section 7).

Slickensides that might correlate with faulting were not found.

Most of the discussion of fault displacement herein focuses on the dextral offset along the principle trace of the Sargent fault NWS. Dip-slip displacement may also be present, as shown in Fig. 5. and as discussed in Section 8 under the heading *Dip-slip fault offset*.

Groundwater. Groundwater is perched atop the buried bedrock surface, i.e., the Kus–Qoa₁ contact. This groundwater level is responsible for the presence of Swanson Creek above (southwest of) the falls. It also produces numerous ephemeral springs along the contact where it is exposed in east-facing slopes adjacent to the falls, as shown in Fig. 13. These springs were observed flowing in early 2019, following abundant winter rainfall, but not in late 2018, following a typical months-long seasonal (summer) drought. This concentration of springs on east-facing slopes is consistent with the gentle eastward dip of the Kus–Qoa₁ contact described earlier.

7. Neotectonic geomorphology

Eight selected sets of distinct neotectonic geomorphologic features are described below in order from west to east. These locations are marked in Fig. 5.

Feature 1: linear hillside. Feature 1 is a northeast-facing hillside that is more or less planar and straight for a distance of about 100 m. Its strike matches that of the Sargent fault where it is exposed to the southeast, near Lower Swanson

Creek Falls (see Feature 2, below). Thus, this linear hillside is clearly a fault-controlled geomorphic feature. Cretaceous sandstone is exposed in the slope above (south of) Uvas Creek Trail. Boulderly slopewash derived from the younger and topographically higher deposits of unit Qoa₁ obscures the traces of both the Kus–Qoa₁ contact and the Sargent fault. The exact locations of the contact and fault here and to the northwest remain uncertain in the absence of safe direct access via belaying equipment. Dip-slip (SW-side-up) displacement on a branch of the Sargent fault that coincides with Uvas Creek's channel may have exerted the tectonic control responsible for this linear hillside.

Feature 2: falls, bowl, etc. Feature 2 is dominated by Lower Swanson Creek Falls, where Swanson Creek plunges some 6 m into a plunge pool. The geometry of the falls suggests that dip-slip displacement (SW side up) of roughly 6 m occurred on the Sargent fault, but not necessarily here; more likely, it occurred to the northwest, at the location of Uvas Creek, as shown in Fig. 5 and discussed in Section 8 under *Dip-slip fault offset*. A topographic bowl that half-way encompasses the falls has been created by some complex combination of differential erosion controlled largely by Neogene–Quaternary tectonic shearing, conventional stream erosion, late Quaternary (Holocene?) dextral tectonic offset, and recent landsliding. The recent landsliding may be driven by the groundwater perched on the buried bedrock surface, as shown by the springs emanating from the exposed Kus–Qoa₁ contact here. The scar left by recent sliding of slope material (involving both Kus bedrock and overlying Qoa₁) is fresh and steep, i.e., nearly vertical to overhanging, and thus is young, perhaps several years to several decades old. The landslide material that fell into and around the plunge pool has been mostly washed away by Swanson Creek. At the top of the landslide scar and beyond (to the west), the fault trace appears to be marked by a small topographic discordance (bench?), as seen in Fig. 13.

Feature 3: knife-edge ridge. Feature 3 is a northwest-oriented knife-edge ridge that is about 7 m tall (Fig. 14). Its flanks are steep and, in places, vertical to overhanging. This ridge, if it has been entrained in the most-recent dextral offset along the Sargent fault, may have deflected Swanson Creek eastward a few meters. If so, it may constitute a shutter ridge, one younger than the shutter ridge of Feature 6 (discussed below). Alternately, its presence may be explained merely by differential erosion in a scenario in which the waterfall eroded away the less-resistant sheared shale within the shear zone in front of it, and Swanson Creek carved a path of least resistance for itself, i.e., around the more-resistant rock of the ridge and to the right (east). The extremely youthful features of this ridge and the precariously rooted trees at the top that help hold the ridge crest in place will not be present for more than a short time, i.e., a few years.

Feature 4: cliff, bench, and contorted microtopography. Feature 4 hosts a small northeast-facing bedrock cliff (Fig.

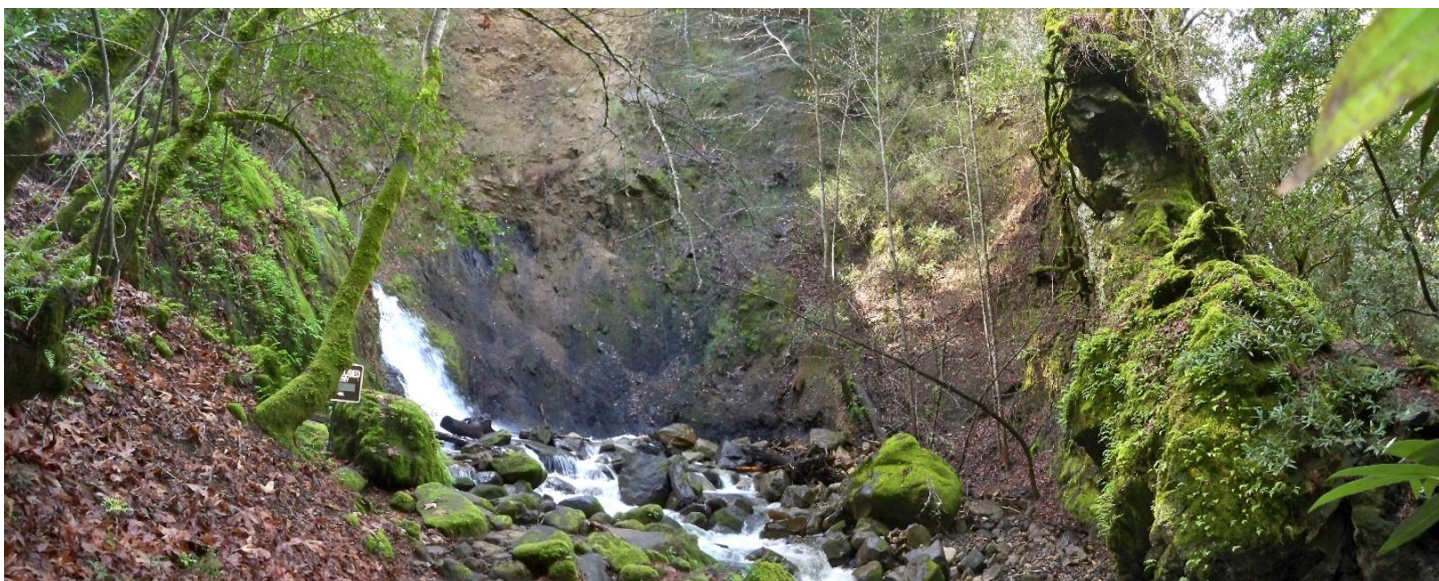


Figure 14. The falls (left), eroded bowl (center), and knife-edge ridge (right). This view is to the west, into the bowl, from the lower end of Swanson Creek Trail. The knife-edge ridge extends about 20 m toward the viewer. The visible part of Lower Swanson Creek Falls is about 3 m tall. A portion of this view is shown in Fig. 13.

15) and, below, a tiny bench a few meters wide with relict contorted microtopography. These features are too small to depict in Fig. 5. The cliff shown in Fig. 15 is about 2 m tall by 3½ m long, strikes N80°W, and dips 90° to 65°S (i.e., overhanging). Its face is rough and displays no striations. On the east end of the cliff, the plane between Kus bedrock on either side (i.e., the plane of the cliff extending into bedrock) is characterized by a zone of fractures that are open, with openings up to 1 cm wide. On the west end, two similar zones of open fractures extend southward into the cliff. The ground at the foot of the cliff appears to be a remnant hillside bench on which a tiny drainage system began to develop before Swanson Creek below (to the north) eroded away the ground below.

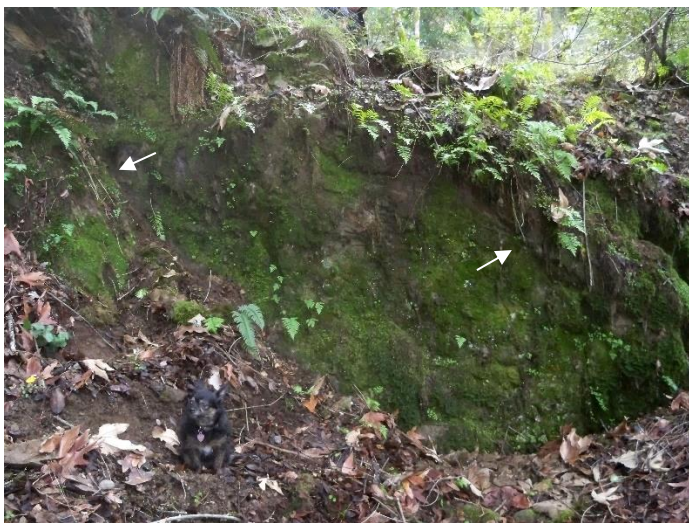


Figure 15. Cliff at Feature 4, viewed looking south. Small black and tan dog, for scale, is 23 cm tall. At least two zones of open fractures, marked by white arrows, extend to the left, eastward (left arrow), and into the cliff, away from the viewer, southward (right arrow).

Feature 5, hanging valley. Feature 5 is a small, anomalously shaped valley about 50 m long by 30 m wide. It is bounded on the north by Feature 6 (shutter ridge, described below) and on the south by a tall, 50° flank of the park office terrace, underlain by Qoa₁. The valley's floor, which is more-or-less planar, lies at about Elev. 1020. Because this floor elevation essentially matches that of the Kus–Qoa₁ contact exposed at the falls, the valley's paleofloor, consisting of Kus bedrock, may underlie the ground surface and unit Qoa₃ at a depth of merely 2 m. The east end of the hanging valley is marked by an abrupt increase in gradient, which likely marks the location of a paleowaterfall/cascade. The paleochannel of Swanson Creek within the hanging valley is not clearly delineated. Its latest alignment probably was along the south side of the hanging valley (Fig. 5). Such an alignment would have produced the shortest route and thus the steepest gradient of the paleocreek toward its junction with the paleowaterfall.

Feature 6, shutter ridge. Feature 6 is a small, anomalous, elongated ridge that rises about 7 m above the hanging valley (on the south) and 20 m above Uvas Creek (to the north). This ridge is clearly a shutter ridge that deflected paleo-Swanson Creek some 75 m (±15 m) eastward (Fig. 5). The south-facing flank of the ridge bounding the hanging valley is linear and strikes N60°W and dips 40–50° SW (Fig. 16). The lower flanks of the ridge, up to about Elev. 1027 ft, are underlain by unit Kus, and the ridge crest above is underlain by unit Qoa₁. The Kus–Qoa₁ contact is well exposed next to Swanson Creek Trail on the east end of the ridge. Note the 3-m difference between elevations of the Kus–Qoa₁ contact across the fault, at about Elev. 1027 ft on the shutter ridge and about Elev. 1018 ft on the southern block, consistent with the 2 m of vertical separation (NE side up) exposed at Feature 2.

Feature 7: sinuous relict ravine. Feature 7 is a narrow, sinuous, steeply plunging ravine carved by the beheaded portion of Swanson Creek. The ravine begins on the south at the downstream (east) end of the hanging valley. There, the extremely steep gradient indicates that there might have been a waterfall or cascade some 3 to 6 m tall where paleo-Swanson Creek plunged off this end of the hanging valley. Directly downstream, the paleochannel is deflected to the right (east) by exposed steep faces composed of resistant Kus bedrock at the base of the shutter ridge (Feature 6). A short distance down, the paleochannel is bounded by a north-facing cliff composed of exposed resistant Kus sandstone and conglomer-



Figure 16. Shutter ridge of Feature 6, viewed northwestward along strike from its southeast end. Note the slope gradient of 40–50° to the left (southeast). Swanson Creek Trail passes left to right in the foreground.

ate. This cliff is 5 m tall by 10 m long, strikes N75°W, and is vertical to overhanging (Fig. 17). A few meters uphill and east of the paleochannel, at about Elev. 1010 ft, there is a similar,



Figure 17. Large north-facing cliff, viewed looking south from a distance of about 10 m. Clipboard (center) for scale.

smaller north-facing bedrock cliff that is 1 m tall by 3½ m long, strikes N75°W, and is vertical to overhanging (Fig. 18). Both cliffs, although planar, are rough and display no striations. Another short distance downstream, the paleochannel is deflected to the left (northwest) by sandstone bedrock, some of which is exposed. Finally, the paleochannel is deflected



Figure 18. Small north-facing cliff, viewed looking southeast. Clipboard for scale.

sharply to the right (northeast), evidently by a 2–3-m-tall debris-flow lobe consisting of unit Qoa₂.

The floor of the ravine was dry in late 2018. In early 2019, at the peak of the rainy season, following roughly a meter of recent rainfall, there was several liters per minute of stream flow within the lower ¾ of the ravine. This ephemeral stream is clearly too weak to move any boulders within the ravine; it is fed only by local groundwater. This low flow supports the notion that units Qoa₃ and Qoa₂ are relict deposits.

Feature 8: linear hillside. Feature 8 is another linear hillside. The northeast-facing hillside here is distinctly linear for a distance of some 50 m. Here, at about Elev. 1050 ft, there is also a linear northeast-facing slope about 2 m tall by 30 m long that may be a fault scarp modified by grading for a building pad in the late 19th century or early 20th century. To the east, the grade of Croy Road is particularly steep, suggesting that the road traverses (obliquely) a northeast-facing fault scarp.

8. Neotectonic geomorphologic development

The neotectonics of the Swanson locality are one process in an extremely complex set of interacting processes that include plate-to-plate movement; orogeny; regional and local faulting and folding; stream erosion, lateral planation, and aggradation; mass slope movements (landsliding); and typical hillside and fluvial geomorphic evolution, which include differential resistance to erosion. The local processes are not yet fully disentangled and understood separately, nor do the existing data allow for unequivocal modeling of the overall geomorphic evolution of the Swanson locality. Particularly perplexing is the location and timing of dip-slip (SW-side-up) offset along the Sargent fault. Nevertheless, the findings described above are used to develop the following tentative timeline of dextral offset along the Sargent fault NWS and associated geomorphic development within the Swanson locality.

Deposition of large alluvial fan, unit Qoa₁. Unit Qoa₁ was evidently deposited on an extensive, gently eastward-sloping triangular bedrock surface created by lateral planation by Swanson and Uvas Creeks (Fig. 3) some time in the Pleistocene.

Both this extensive bedrock surface and the extensive thick alluvial aggradation represented by unit Qoa₁ are anomalous. Previous mapping by others (e.g., McLaughlin et al., 2001) shows no other significant analogous stream terrace deposit alongside Uvas Creek or its tributary streams within a distance of several kilometers. Swanson Creek's drainage basin is small, and that of Uvas Creek upstream is not much larger.

However, consider a scenario in which this bedrock surface and unit Qoa₁ represent a crude ancestral version of the hanging valley, enlarged by a factor of about ten. In this scenario, based on the extent of unit Qoa₁, Swanson Creek experienced roughly 700 m of dextral offset, perhaps beginning at 250–300 ka, i.e., in the middle Pleistocene. A shutter ridge (present location unclear), analogous to the one in Feature 6 but much larger, was responsible for offsetting the creek (analogous younger set of processes described under *Dextral fault offset*, below). Due to this blockage, lateral planation by Swanson Creek produced the bedrock surface (a strath terrace), and the decrease in stream gradient led to alluvial aggradation that produced unit Qoa₁. This shutter-ridge explanation is supported by two observations: (1) The ratios of the east–west length to thickness of units Qoa₃ and Qoa₁ are similar: 75 m / 2 m = 38 for unit Qoa₃, and 700 m / 25 m = 28 for unit Qoa₁. (2) Qoa₁ was not mapped north of Uvas Creek.²

Incision of alluvial fan. Sometime in the late Pleistocene, the cause(s) responsible for deposition of unit Qoa₁ ended. Perhaps the large shutter ridge described above was worn down or was down-dropped by NE-side-down slip on the Sargent fault (see *Dip-slip fault offset*, below). Consequently, a rejuvenated Swanson Creek, perhaps following its ancestral course, incised a relatively straight, narrow ravine down through unit Qoa₁ to bedrock, thereby separating the campground terrace from the park office terrace. (Note that this large-scale stream avulsion is analogous to the later, smaller-scale stream avulsion described below under *Avulsion of Swanson Creek*.) Downward incision through this relatively soft alluvium might have been rapid, but its downward extent was eventually limited by the resistant sandstone bedrock surface underlying unit Qoa₁. The alignment of the rejuvenated creek may have roughly coincided with that of present-day Swanson Creek.

The large volume of debris-flow material represented by unit Qoa₂ along with its lowlying topographic position suggest that the derivation of source material from unit Qoa₁ and its

redeposition by rejuvenated paleo-Swanson Creek occurred during a late phase of terrace incision but while the incision was still relatively active. The large volume of debris-flow material evidently formed a small alluvial fan at the paleoconfluence of Swanson and Uvas Creeks. This fan deflected Uvas Creek about 20 m to the north, creating the meander evident in Fig. 5.

Dip-slip fault offset. Displacement with some dip-slip component along the Sargent fault (SW side up) likely occurred somewhere in the Swanson locality. Exactly where this displacement occurred is unclear, and when it occurred is even less clear. This presence of dip-slip displacement is based on the regional mapping of the Sargent fault by previous workers (see Section 5) and on local geomorphic clues. These geomorphic clues consist of three sets of features: (1) the paleowaterfall and present-day Swanson Creek falls, (2) the linear slopes (Features 1 and 8) and alignment of Uvas Creek, and (3) the contrast in topography on the south side of Uvas Creek versus the north side.

The position and geometry of the paleowaterfall and present-day falls suggest late Quaternary SW-side-up fault slip of some 6 m, judging from the heights of the waterfalls. The steep linear northeast-facing slopes and the straight alignment of adjacent Uvas Creek are suggestive of, respectively, a northeast-facing fault scarp and a positioning of the stream alignment along the scarp's base, i.e., along a lowlying path of least resistance. The contrast in topography consists of slopes that tend to be noticeably steeper and taller on the south side of Uvas Creek than on the north side.

This dip-slip displacement, therefore, might be located along a northwestern branch of the Sargent fault, essentially coinciding with the alignment of Uvas Creek. This conjectured fault is shown in Fig. 5 as a queried, approximately located, mostly concealed fault trace. If dip-slip displacement occurred there, then the waterfalls retreated upstream, perhaps rapidly, some 30–40 m from their original positions, with the retreat perhaps ending at a particularly resistant zone of Kus bedrock.

In an alternative scenario, no late Quaternary dip-slip displacement occurred here, and Uvas Creek merely incised down into the bedrock more deeply than did Swanson Creek, thereby creating the waterfalls, which then underwent their conjectured retreat of 30–40 m.

It seems unlikely that latest Quaternary SW-side-up displacement occurred along the well-defined (southwestern) trace of the Sargent fault. Such displacement is incompatible with the 2 m of NE-side-up separation of the Kus–Qoa₁ contact observed at Swanson Creek Falls. Also, no SW-side-up displacement here was preserved by burial by unit Qoa₁.

large landslides, each measuring nearly 1 sq. km and located 1 km downstream of the Swanson locality (see map by McLaughlin et al., 2001), which might have dammed Uvas Creek.

² Two contributing or alternative causative processes might have been (1) unusually strong erosion within Swanson Creek's drainage basin, perhaps aided by a wetter Pleistocene climate, and (2) two

Dextral fault offset. Dextral offset along the Sargent fault began to slice the shutter ridge (Feature 6) from the campground terrace and move it to the right (east) and alongside the park office terrace. As the shutter ridge moved, Swanson Creek was gradually deflected (offset) to the right (east). The conjectured paleowaterfall/cascade was also offset dextrally. Total stream offset was about 75 m (± 15 m).

The buried top-of-bedrock surface (i.e., Kus–Qoa₁ contact) generally sloped gently eastward, as it apparently does now. This slope set up two conditions within the hanging valley: (1) As horizontal fault slip progressed, rock at a higher elevation on the northern block was juxtaposed against rock at a lower elevation on the southern block; thus, elevated resistant rock of the shutter ridge forced the deflected creek to remain on the southern block, within the hanging valley. (2) The deflected creek was also *able* to remain on the southern block by flowing eastward across an eastward-sloping exhumed bedrock surface. The creek's altered course, therefore, generally remained within (and produced) the hanging valley rather than developing on the northern block, specifically, along the crease where the east end of the shutter ridge meets the scarp bounding the southern block. The paleocreek was able to gradually migrate eastward across the exhumed bedrock surface only by gradually removing a large volume of adjacent soft alluvial material (unit Qoa₁) from the northwest corner of the park office terrace.

Consequently, this 60-m-long segment of the paleocreek, rather than making a sharp, 90° rightward turn at the fault, generally developed a 45° rightward sweep toward the paleowaterfall/cascade (Fig. 5). This lateral sweeping away of older alluvium and rightward migration of the paleocreek were the stream's attempt to maximize its gradient and transport its large sediment load. Downward incision by the creek was negligible, due to the resistant exhumed bedrock surface. Thus, the exhumed Kus–Qoa₁ contact became the surface on which unit Qoa₃ was deposited. The results of all this stream offset and lateral planation were the hanging valley, with its peculiar outline and relatively level floor.

A minor fraction of the dextral stream offset did occur on the northern block. At Elev. 990 ft within the sinuous ravine, the paleocreek evidently made a 90° rightward (eastward) bend and flowed eastward for a distance of some 5–10 m. Perhaps the paleocreek upstream finally lacked sufficient energy to laterally erode the adjacent material of unit Qoa₁ underlying the park office terrace, or the east end of the shutter ridge was worn down, thus degrading its ability to keep the stream on the southern block.

The several small bedrock cliffs or exposures described in Section 7 are candidate fault scarps produced by this dextral fault offset. They include the downslope- (north-) facing cliff at Feature 4 (Fig. 14) and the upslope- (south-) facing bedrock exposure and two downslope- (north-) facing cliffs within the sinuous ravine (Figs. 16 and 17). The orientations of these

cliffs relative to Swanson Creek, the Sargent fault, and the shutter ridge are consistent with a pattern of scarp aspects in a strike-slip setting described by Weldon et al. 1996 (p. 286–287): the rock exposure on the downstream block faces upslope (south), and the cliffs on the upstream block face downslope (north).

The offset of the paleocreek within the hanging valley lengthened this stream segment from about 30 m to 60 m. The segment's gradient was thereby reduced by about one half. The result was local recent stream aggradation, represented by the deposition of unit Qoa₃ within the hanging valley and upstream for a distance of some 100 m, as shown in Fig. 5.

Avulsion of Swanson Creek. The decreased gradient and increased aggradation within the hanging valley set up conditions for the beheading of paleo-Swanson Creek. The landslide on the east end of the hanging valley may have dammed, or at least contributed to the clogging of, paleo-Swanson Creek at this location. The final alluvial deposition (unit Qoa₃) by paleo-Swanson Creek apparently was by way of flooding and debris flows within the hanging valley. If the enigmatic manmade objects (barrel [Fig. 11], pipe) protruding slightly above the ground are indeed components that were naturally entrained within unit Qoa₃, then this deposition occurred in the early 20th century. Some combination of the latest alluvial deposition, the landslide, and the decreased stream gradient and aggradation within the hanging valley caused the avulsion of paleo-Swanson Creek, i.e., its rapid diversion to the west. Swanson Creek now flows within a relatively straight channel toward the falls. This diversion likely represents Swanson Creek's resumption of its pre-offset alignment and, possibly, its ancestral alignment.

Latest dextral stream offset? Below the falls, the knife-edge ridge deflects Swanson Creek about 20 m eastward toward its confluence with Uvas Creek. Much or all of this creek deflection is likely due to differential erosion below the falls. Some or none of this deflection could be due to the ridge's function as a smaller shutter ridge that postdates the movement of the larger shutter ridge of Feature 6. If there was displacement along a younger, secondary trace of the Sargent fault here, then this trace is located a few meters north of the principal trace shown in Fig. 5, and its extensions to the northwest and southeast are not well defined.

9. Timing of offset and paleoseismological implications

Assuming a slip rate of 3 mm/yr (Prescott and Burford, 1976), the offset of about 75 m (± 15 m) occurred over a time period of about 25 ky (± 5 ky). Much of the later portion of this time period likely extended into or spans the Holocene, based on (1) the Holocene paleoearthquakes on the Sargent fault SES documented by Nolan et al. (1995), (2) the historic slip rate of 3 mm/yr documented by Prescott and Burford (1976), and (3) the freshness of certain features at the Swanson locality, par-

ticularly, the tall overhanging cliffs and the contorted microtopography.

The cliffs in the Swanson locality, which are mostly vertical to overhanging and appear to be Holocene fault scarps, range from 3½ to 10 m long. The field data may be insufficient for distinguishing paleoearthquakes among these cliffs/scarps. At a site where “landforms were offset by tens of meters (i.e., from multiple faulting events), ... only slip rates, and not parameters of individual paleoearthquakes” can be deduced in a strike-slip setting (Weldon et al., 1996, p. 285).

Perhaps, however, the two small cliffs at Features 4 and 7 (Figs. 15 and 18, respectively), which are both 3½ m long, could be tentatively attributed to a single paleoevent or to two paleoevents of equal slip. A coseismic displacement of 3½ m, along with Prescott and Burford’s (1976) slip rate of 3 mm/yr, would yield a recurrence interval of 1200 yr. This value matches the recurrence interval of 1200 yr assigned to the Sargent fault by Petersen et al. (1996). See the table, below. Petersen et al. (1996) based this recurrence interval on their review of the work by Nolan et al. (1995).

Nolan et al. (1995) performed trenching and ¹⁴C dating of Holocene alluvial layers offset by the Sargent fault SES. They reported recurrence intervals of 1200 and 1485 yr. They also logged coseismic slips measuring 0.7–0.8 m (and one of 1.7 m) in their trench exposures. These recurrence intervals and coseismic slips led the authors to calculate a slip rate of 0.6 mm/yr, which they acknowledged was unexpectedly low. Perhaps true coseismic slips greater than 0.7 or 1.7 m within rock at depth were attenuated during their upward propagation into

the near-surface Holocene alluvium, or perhaps the rake angles of the striations noted in the trenches, which differed little from horizontal, yielded estimates of strike-slip coseismic paleo-offsets that were too low.³ If so, then the recurrence interval of about 1200 yr documented by Nolan et al. (1995) remains convincing, their near-surface estimates of paleo-offsets were lower than true coseismic paleo-offsets (at depth), and the slip rate of 3 mm/yr reported by Prescott and Burford (1976) remains valid.

Another check is useful. WGNECEP (1996) and Petersen et al. (1996) assigned a maximum event magnitude of 6.8 to the Sargent fault based on its dimensions.⁴ This event magnitude of 6.8 and a conjectured coseismic surface displacement of 3½ m can be compared to similar data from historical earthquakes. Wells and Coppersmith (1994) developed a regression of maximum surface displacements vs. moment magnitudes based on 421 historical earthquake records. A data point of maximum surface displacement = 3½ m and $M = 6.8$ plots on the lower bound of a 95% confidence interval around the regression developed by Wells and Coppersmith (1994).

Clearly, the uncanny “exact match” between a 1200-yr calculated recurrence interval at the Swanson locality and similar values reported elsewhere by others could be largely fortuitous. Several uncertainties should be considered: (1) whether the two 3½-m-long cliffs in question are indeed fault scarps, (2) whether they represent a single paleoevent, (3) whether their measured lengths are accurate or instead are minima due to weathering and coverage by slopewash, and (4) the extent to which this conjectured coseismic slip is exceeded by the true coseismic slip at depth. The fact that the cliffs involve

Table. Slip rates, amounts of coseismic slip, and recurrence intervals assigned to the Sargent fault by various authors. Values in **bold** are based directly on field observations. Other values were based on data from the literature or were calculated.

Slip rate, <i>r</i> (mm/yr)	Coseismic slip, <i>d</i> (m)	Recurrence interval, <i>t</i> (yr)	Study, segment(s) of Sargent fault	Methods and sources
3	—	—	Prescott and Burford (1976), SES	Extensive trilateration survey network
4	—	—	Savage et al. (1979), SES	Extensive trilateration survey network
0.6	0.7–0.8^a	1200–1485	Nolan et al. (1995), SES	¹⁴ C dating of Holocene alluvium layers, <i>r</i> calculated ^b
3	1	330	WGNECEP (1996), both ^d	<i>R</i> from PB76, <i>d</i> (rounded?) from PB76(?), <i>t</i> calculated ^b
3	— ^c	1200	Petersen et al. (1996), both ^d	<i>R</i> from PB76, <i>t</i> from N95
3	3.5	1200	This study, NWS	Lengths of fault scarps in rock, <i>r</i> from PB76, <i>t</i> calculated ^b

Abbreviations: SES = southeast segment, NWS = northwest segment, PB76 = Prescott and Burford (1976), N95 = Nolan et al. (1995).

a. Range of three of four paleoseismic events observed in trenches; penultimate event measured 1.7 m.

b. Calculations were performed using the equation $t = d / r$ and simple algebraic derivations thereof.

c. Coseismic slip not given; calculation implies or requires that this value would be 3.6 or 4 m.

d. These two studies were essentially meta-analyses wherein findings regarding the Sargent fault SES were extrapolated to the entire length of the fault.

³ Nolan et al. (1995) speculated that additional slip must be transferred to another fault between their trench site and the trilateration array of Prescott and Burford (1976), located about 13 km to the northwest.

⁴ Specifically, based on a length of 53 km, down-dip width of 12 km, and an empirical relationship between magnitude and rupture area (length × width). This event magnitude is derived independent of any event slip, slip rate, or recurrence interval.

bedrock rather than thick soft alluvium may minimize this fourth uncertainty.

Local data for calculating a slip rate are lacking because no dates are assigned to any of the features or offsets in the Swanson locality. Charcoal has not yet been observed in exposures of the Quaternary deposits, and thus ^{14}C dating of the deposits and fault offsets is possible only with further detailed observations. Future trench exploration is not possible in the Swanson locality due to its location in Uvas Canyon County Park, where disturbance of natural features is prohibited. However, Swanson Creek has created extensive fresh vertical exposures of unit Qoa₃, and unit Qoa₂ is covered only by minimal thicknesses of moss. If charcoal and ^{14}C dates were obtained from unit Qoa₂ or from the bottom of unit Qoa₃, then the beginning of the 75 m of stream offset could be dated. Assuming that (1) all the foregoing mapping and interpretation of the Quaternary geology within the Swanson locality are correct and that (2) the slip rate of 3 mm/yr along the Sargent fault (Prescott and Burford, 1976) is correct, then ages of roughly 27 ka of unit Qoa₂ and 25 ka of the bottom of unit Qoa₃ would be predicted.

10. Conclusions, limitations, and further discussion

This locality at the confluence of Uvas and Swanson Creeks hosts a previously undocumented set of neotectonic geomorphic features indicating significant well-defined late Quaternary dextral surface offset along the Sargent fault NWS. All of the features, evaluated as a set, fit various aspects of models of strike-slip neotectonism in a mountain-front setting described by Weldon et al. (1996). The locality may be somewhat atypical, however, by virtue of the very high-energy fluvial setting at the confluence of two tightly confined streams.

The latest Quaternary surface offset measures about 75 m (± 15 m). This finding represents the first field identification and quantification of latest Quaternary surface offset along the Sargent fault NWS.⁵ This offset spanned about 25 ky (± 5 ky) and probably extends into the Holocene. Two of the cliffs likely are fault scarps involving rock, and if so, their $3\frac{1}{2}$ -m horizontal lengths may represent paleoevents that suggest confirmation of a 1200-yr recurrence interval, reported by others, associated with $M = 6.8$ earthquakes along the Sargent fault.

Previously, the Sargent fault NWS had been mapped as concealed beneath (predating) an extensive alluvial deposit for a distance of 1.3 km along strike within and beyond the Swanson locality; the fault's location, therefore, was only moderately well constrained. The alignment of geomorphic features constrains the principle young(est?) trace within the Swanson locality to a zone a few meters wide, and where the offset of Pleistocene alluvium is prominently exposed next to the falls, the trace can be located to within 1 m. The overall northeast

dip of the Sargent fault NWS, based on its exposed trace at the Swanson locality, tends to confirm the northeastward dip of this fault segment above a depth of 2 km conjectured by Zhang et al. (2018; Fig. 4). Although pre-Qoa₁ dip slip is evident, the slip vector of the latest Quaternary (post-Qoa₁) fault displacement appears to be purely strike-slip.

This study was hampered by the limited detail of the existing topographic base map, whose contour interval is 10 ft (3.3 m) and is not reliable in critical locations. A base map with a tighter contour interval, e.g., 2 ft. (0.7 m), would allow for more-precise mapping and study of the neotectonic features.

The findings from this locality could be combined with findings from undocumented similar localities elsewhere along the Sargent fault NWS. A cursory examination of 10-ft- (3.3-m-) contour topographic maps suggests that several other localities within the Loma Prieta quadrangle along the trace of the Sargent fault NWS may host similar sets of neotectonic features. Two such localities are at lat. 37.1034 N, long. -121.8410 W, and lat. 37.1006 N, long. -121.8331 W. The area of Sveadal could yield similar data.

The findings from this study are consistent with, and thus likely will not affect, existing local development planning and regional seismic-hazard planning. A zone straddling the Sargent fault NWS wherein investigation for active ground-surface rupture is required to construct dwellings has been delineated by the Santa Clara County Planning Department. In addition, findings from the Sargent fault SES were previously extrapolated to the Sargent fault NWS to yield a combined, single source of potential seismic ground shaking, namely, the Sargent fault (Petersen et al., 1996), for inclusion in seismic hazard planning in regional structural design.

References

- Bryant, W.A., compiler, 2000a, Fault number 58a, Sargent fault zone, northwestern section, in Quaternary fault and fold database of the United States: U.S. Geological Survey, https://earthquake.usgs.gov/cfusion/qfault/show_report_AB.cfm?fault_id=58§ion_id=a.
- Bryant, W.A., compiler, 2000b, Fault number 58b, Sargent fault zone, southeastern section, in Quaternary fault and fold database of the United States: U.S. Geological Survey website, https://earthquake.usgs.gov/cfusion/qfault/show_report_AB.cfm?fault_id=58§ion_id=b.
- Dibblee, T.W., and Brabb, E.E., 1980, Preliminary geologic map of the Loma-Prieta quadrangle, Santa Cruz and Santa Clara Counties, California: U.S. Geological Survey, Open-File Report OF-80-944, scale 1:24,000.

⁵ Aside from several centimeters of offset observed at the northwesternmost end of the fault following the 1989 Loma Prieta earthquake (McLaughlin and Clark, 2004).

- Dibblee, T.W., and Minch, J.A., 2005, Geologic map of the Loma Prieta quadrangle, Santa Clara and Santa Cruz Counties, California: Dibblee Geological Foundation Map DF-167, https://ngmdb.usgs.gov/Prodesc/proddesc_73805.htm.
- Dietz, L.D. and Ellsworth, W.L., 1990, The October 17, 1989, Loma Prieta, California earthquake and its aftershocks: geometry of the sequence from high-resolution locations: *Geophysical Research Letters*, vol. 17, p. 1417–1420, <http://digitalcommons.unl.edu/usgsstaffpub/371>.
- Graymer, R.W., 1997, Geology of the southernmost part of Santa Clara County, California; a digital database: U.S. Geological Survey Open-File Report 97-710, <https://pubs.usgs.gov/of/1997/of97-710/>.
- Kilb, D., and Hardebeck, J.L., 2006: Fault parameter constraints using relocated earthquakes: a validation of first-motion focal-mechanism data: *Bulletin of the Seismological Society of America*, vol. 96, p. 1140–1158.
- McLaughlin, R.J., 1973, Geology of the Sargent fault zone in the vicinity of Mount Madonna, Santa Clara and Santa Cruz Counties, California. San Jose State University [San Jose, California] master's thesis, 131 p.
- McLaughlin, R.J., 1974, The Sargent-Berrocal fault zone and its relation to the San Andreas fault system in the southern San Francisco Bay region and Santa Clara Valley, California: *Journal of Research of the U.S. Geological Survey*, vol. 2 (5), p. 593–598.
- McLaughlin, R.J., Clark, J.C., and Brabb, E.E., 1988, Geologic map and structure sections of the Loma Prieta 71/2' quadrangle, Santa Clara and Santa Cruz Counties, California: U.S. Geological Survey Open-File Report OF-88-752.
- McLaughlin, R.J., Langenheim, V.E., Jachens, R.C., Jayko, A.S., Stanley, R.G., and Valin, Z.C., 1997, Neogene transpressional range-front deformation, southwestern Silicon Valley, San Francisco Bay region, California [abs.]: EOS, Transactions of the American Geophysical Union, 1997 Annual Fall Meeting, vol. 78, (46), p. F436
- McLaughlin, R.J., Clark, J.C., Brabb, E.E., Helley, E.J., and Colon, C.J., 2001, Geologic maps and structure sections of the southwestern Santa Clara Valley and southern Santa Cruz Mountains, Santa Clara and Santa Cruz Counties, California: U.S. Geological Survey Miscellaneous Field Studies Map MF-2373.
- McLaughlin, R.J., and Clark, J.C., 2004, Stratigraphy and structure across the San Andreas fault zone in the Loma Prieta region and deformation during the earthquake, in Wells, R.E., *The Loma Prieta, California, earthquake of October 17, 1989—geologic setting and Crustal Structure*: U.S. Geological Survey Professional Paper 1550E, p. 5–48.
- McLaughlin, R.J., Clark, J.C., Brabb, E.E., Helley, E.J., and Wentworth, C.M., 2004, Geologic map of the Loma Prieta region, California, in Wells, R.E., *The Loma Prieta, California, earthquake of October 17, 1989—geologic setting and Crustal Structure*: U.S. Geological Survey Professional Paper 1550E, plate 1.
- Nolan, J.M., Zinn, E.N., and Weber, G.E., 1995, Paleoseismic study of the southern Sargent fault, Santa Clara and San Benito Counties, California: Unpublished U.S. Geological NEHRP Final Technical Report 1434-94-G-2466.
- Petersen, M.D., Bryant, W.A., Cramer, C.H., Cao, T., Reichle, M.S., Frankel, A.D., Lienkaemper, J.J., McCrory, P.A., and Schwartz, D.P., 1996, Probabilistic seismic hazard assessment for the State of California: U.S. Geological Open-File Report 96-706.
- Prescott, W.H., and Burford, R.O., 1976, Slip on the Sargent fault: *Bulletin of the Seismological Society of America*, vol. 66, p. 1013–1016.
- Santa Clara County, SCVWD, USGS, and SFEI, 2017, Santa Clara County Map: interactive product prepared by County of Santa Clara [California] Geographic Information Services, <https://ges.sccgov.org/discovergis/sccmap>, accessed December 2018.
- Santa Clara County Parks, 2015, Uvas Canyon [County Park]: park brochure prepared by County of Santa Clara Parks and Recreation Department, Los Gatos, California.
- Savage, J.C., Prescott, W.H., Lisowski, M., and King, N., 1979, Geodolite measurements of deformation near Hollister, California, 1971-1978: *Journal of Geophysical Research*, v. 84, no. B13, p. 7599-7615.
- Turner, R.C., Nadeau, R.M., and Burgmann, R., 2013, Aseismic slip and fault interaction from repeating earthquakes in the Loma Prieta aftershock zone: *Geophysical Research Letters*, vol. 40, p. 1079–1083.
- Weldon, R.J., McCalpin, J.P., and Rockwell, T.K., 1996, Paleoseismology of strike-slip tectonic environments: Chapter 6 (p. 271–329) in McCalpin, ed., *Paleoseismology*, Academic Press, San Diego.
- Wells, D.L., and Coppersmith, K.J., 1994, New empirical relationships among magnitude, rupture length, rupture width, rupture area, and surface displacement: *Bulletin of the Seismological Society of America*, vol. 84, no. 4, p. 974–1002.
- Wentworth, C.M., Blake, M.C., McLaughlin, R.J., and Graymer, R.W., 1999, Preliminary geologic map of the San Jose 30 X 60-minute quadrangle, California: a digital database: U.S. Geological Survey Series and Number: Open-File Report OF-98-795.
- WGNEP (Working Group on Northern California Earthquake Potential), Lienkaemper, J.J., and Schwartz, D.P., co-chairs, with twenty-seven others, 1996, Database of potential sources for earthquakes larger than magnitude 6 in northern California: U.S. Geological Survey Open-File Report 96-705.
- Zhang, E., Fuis, G.S., Catchings, R.D., Scheirer, D.S., Goldman, M., and Bauer, K., 2018, Reexamination of the subsurface fault structure in the vicinity of the 1989 moment-magnitude-6.9 Loma Prieta earthquake, central California, using steep-reflection, earthquake, and magnetic data: U.S. Geological Survey Open-File Report 2018-1093.

Appendix — Changes to cultural features

Shown below is a timeline of changes to cultural features based on reviews of historical U.S. Geological Survey topographic quadrangle maps available online and aerial photographs available at the U.S. Geological Survey in Menlo Park, California.

Of particular interest is an unpaved road that is shown crossing the Swanson locality in the topographic maps with 1968 photorevisions (maps dated 1969, 1975, and 1986), as shown in Fig. A-1, but not in earlier or later (1994) topographic maps. The slopes in the locality (e.g., alongside Swanson Creek) are far too steep for practical road construction anywhere except directly adjacent to Uvas Creek. Perhaps such a road segment alongside Uvas Creek, if it was present, was washed away by flood waters. Alternately, perhaps a road segment connecting Croy Road to the campground terrace and passing through the Swanson locality never existed. Although the tree canopy cover is dense, the aerial photographs show no evidence anywhere of such a road. No remnants of any such road are visible in the field, based on observations everywhere along the mapped alignment, including areas in and far above the reach of flood waters. Perhaps a hiking trail, something that partly coincided with present-day Uvas Creek Trail, was erroneously shown as an unpaved road in the 1968 photorevision of the topographic map; the maps containing 1968 photorevisions state that those photorevisions were not field checked.

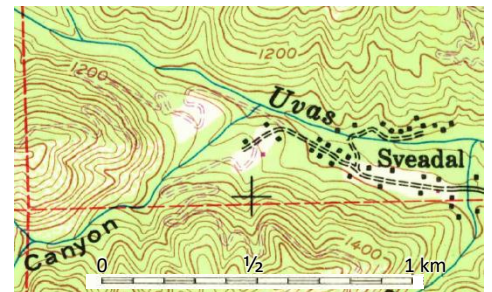
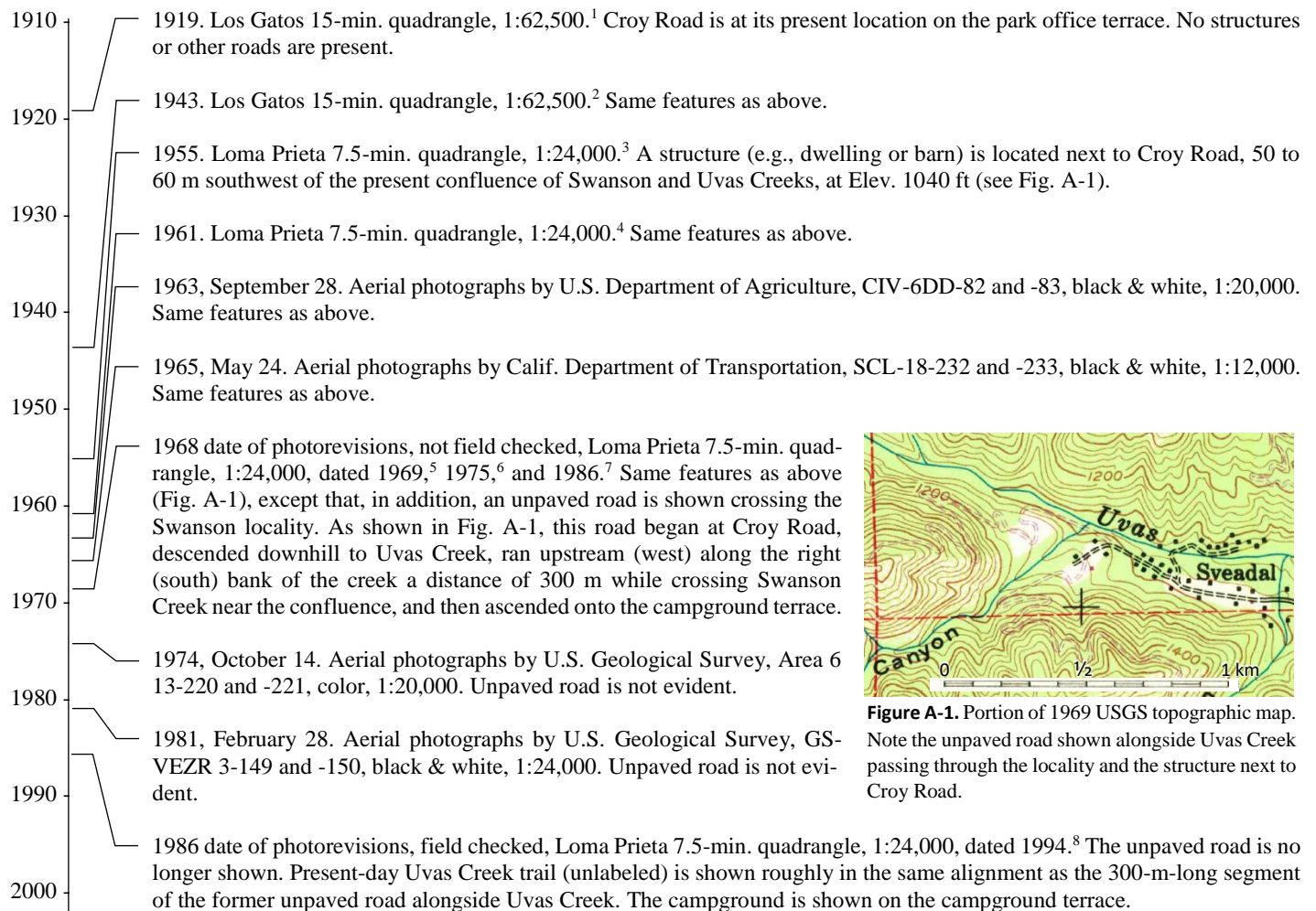


Figure A-1. Portion of 1969 USGS topographic map. Note the unpaved road shown alongside Uvas Creek passing through the locality and the structure next to Croy Road.

¹ https://prd-tnm.s3.amazonaws.com/StagedProducts/Maps/HistoricalTopo/PDF/CA/62500/CA_Los%20Gatos_298061_1919_62500_geo.pdf

² https://prd-tnm.s3.amazonaws.com/StagedProducts/Maps/HistoricalTopo/PDF/CA/62500/CA_Los%20Gatos_298062_1943_62500_geo.pdf

³ https://prd-tnm.s3.amazonaws.com/StagedProducts/Maps/HistoricalTopo/PDF/CA/24000/CA_Loma%20Prieta_292455_1955_24000_geo.pdf

⁴ https://prd-tnm.s3.amazonaws.com/StagedProducts/Maps/HistoricalTopo/PDF/CA/24000/CA_Loma%20Prieta_292456_1955_24000_geo.pdf

⁵ https://prd-tnm.s3.amazonaws.com/StagedProducts/Maps/HistoricalTopo/PDF/CA/24000/CA_Loma%20Prieta_292457_1955_24000_geo.pdf

⁶ https://prd-tnm.s3.amazonaws.com/StagedProducts/Maps/HistoricalTopo/PDF/CA/24000/CA_Loma%20Prieta_292458_1955_24000_geo.pdf

⁷ https://prd-tnm.s3.amazonaws.com/StagedProducts/Maps/HistoricalTopo/PDF/CA/24000/CA_Loma%20Prieta_292452_1955_24000_geo.pdf

⁸ https://prd-tnm.s3.amazonaws.com/StagedProducts/Maps/HistoricalTopo/PDF/CA/24000/CA_Loma%20Prieta_292453_1955_24000_geo.pdf